NTNU
Norwegian University of
Science and Technology

Monte Carlo Finite Volume Methods For Hyperbolic Conservation Laws With Uncertain Initial Data

Jon Christian Espeland Halvorsen
TMA4500: Industrial Mathematics,
Specialization Project

December 2015

Preface

This thesis is written for *TMA4500: Industrial Mathematics, Specialization Project* as a part of my Master of Science degree at NTNU. I would like to thank my supervisor Ulrik S. Fjordholm for a tremendous amount of help and guidance throughout the semester.

Abstract

Using standard Monte Carlo methods we develop a numerical solver for conservation laws with random initial data. The underlying solver is a Rusanov method, based on a finite volume method. We take a closer look at Burgers' equation and for simple test problems numerical accuracy and convergence will be discussed. Statistical properties of the solution, like the mean, variance and second moment are calculated. More advanced problems, like a sine with uncertain phase or amplitude, will also be presented and solved numerically. The numerical method is well suited for parallelism and is implemented with support for using multiple CPU's at the same time. We will briefly discuss what can be done to speed up processing, as the Monte Carlo method converges rather slowly.

Contents

1 Conservation Laws **1**
1.1 Introduction to Conservation Laws 1
1.2 Examples of Conservation Laws 1
1.3 Properties of Conservation Laws 2
1.4 Finite volume scheme 4
1.5 Approximate Riemann solver 5
1.6 Lax-Friedrichs scheme 6
1.7 Rusanov scheme 6

2 Monte Carlo methods **7**

3 Conservation Laws with uncertain initial data **9**
3.1 Monte Carlo Rusanov 9
3.2 Uncertain shock location 9
3.3 Example on uncertain shock location 10

4 Numerical experiments **13**
4.1 Discontinuous initial data 13
4.2 Numerical Monte Carlo method 14
4.3 Discontinuous initial data with skewed cutoff point 14
4.4 Discontinuous initial data with multiple Riemann problems . . 17
4.5 Stochastic amplitude 19
4.6 Stochastic phase 20

5 Conclusion and further work **23**

1 Conservation Laws

In this section conservation laws and numerical methods for them be presented. For more in-depth knowledge and understanding of the subject we refer to Holden and Risebro [1]. For other details the lecture notes by S. Mishra [2] is a good resource.

1.1 Introduction to Conservation Laws

Consider a domain $\Omega \subset \mathbb{R}^n$ and a quantity of interest u that is defined in all points $x \in \Omega$. In conservation laws, this quantity typically is a temperature, a pressure or a density. For a fixed sub-domain $\omega \subset \Omega$ of any size, the rate of change of u over time is equal to the total amount of u produced (or destroyed) inside ω and the flux across the boundaries. An integral representation of this could be

$$\frac{d}{dt}\int_\omega u dx = -\underbrace{\int_{\delta\omega} F \cdot \nu d\sigma(x)}_{\text{flux}} + \underbrace{\int_\omega S dx}_{\text{source or sink}},$$

with ν being the outward normal, $d\sigma(x)$ being the surface measure, F and S being the flux and source. Simplifying this integral by using the Gauss divergence theorem we obtain

$$\frac{d}{dt}\int_\omega u dx + \int_\omega \text{div}(F) dx = \int_\omega S dx.$$

Since this holds for all subdomains $\omega \subset \Omega$, using an infinitesimal ω obtains the following differential equation, known as a *balance law*:

$$\partial_t u + \text{div}(F) = S \qquad \forall (x,t) \in (\Omega, \mathbb{R}_+).$$

If the source (or sink) is zero, we classify this is a conservation law (since u only changes by flux entering or leaving the domain) and it takes the form

$$\partial_t u + \text{div}(F) = 0 \qquad \forall (x,t) \in (\Omega, \mathbb{R}_+). \tag{1.1}$$

1.2 Examples of Conservation Laws

The **scalar transport equation**

$$\partial_t u + \text{div}(a(x,t)u) = 0 \tag{1.2}$$

governs flow over a velocity field $a(x,t)$. If we let u be a concentration of a pollutant in the air, wind will generate the velocity field $a(x,t)$ and the pollutant will be transported with the wind. In a simple case where we consider one dimension and the velocity field is constant, (1.2) reduces to

$$\partial_t u + a\partial_x u = 0,$$

which is often called the transport or **advection equation**.

Given a metal rod that is heated in the center, you would assume that the heat spreads out and in time you get a uniform heat distribution on the rod. For a general medium this diffusion is described by Fick's law:

$$F(u) = -k\nabla u,$$

where k is the conductivity tensor for the medium and $F(u)$ is the flow or the diffusion. Since heat flows from hotter to colder zones we get a minus sign. Plugging this into the general conservation law (1.1) we get

$$\partial_t u - \operatorname{div}(k\nabla u) = 0,$$

which is called the **heat equation**. This equation governs the transportation of heat over time. The heat equation can also model particle diffusion, Brownian motion and a lot of other equations can be reduced to it. The heat equation is a second order partial differential equation. From here and out we only look at first order scalar partial differential equations.

1.3 Properties of Conservation Laws

We look at the first order scalar conservation law

$$\partial_t u + \partial_x f(u) = 0. \tag{1.3}$$

Since the solution (or even the initial data) do not need to be smooth, we multiply with any test function $\phi \in C_c^1(\mathbb{R} \times \mathbb{R}^+)$ and integrate by parts to get

$$\int_{\mathbb{R}\times\mathbb{R}^+} u\partial_t\phi + f(u)\partial_x\phi dxdt + \int_{\mathbb{R}} u_0(x)\phi(x,0)dx = 0.$$

The function $u \in L^1(\mathbb{R} \times \mathbb{R}^+)$ that solves this equation for any ϕ we denote a weak solution to (1.3).

To have uniqueness for weak solutions we need to enforce an *entropy condition*. An example could be the *Lax entropy condition*,

$$f'(u^-(t)) > s(t) > f'(u^+(t)), \tag{1.4}$$

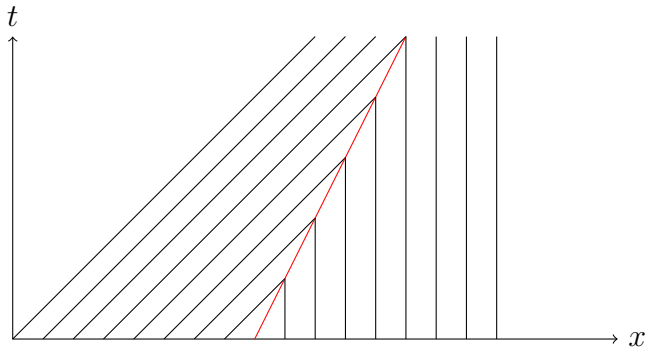

Figure 1: Characteristics of a shock solution.

where s(t) is the shock speed while $u^{\pm}$ is the states on either side of the shock. More general entropy condition can also be used. A weak solution satisfying some entropy condition we call an entropy solution.

The solutions of simple conservation laws can be constructed using the method of characteristics. For some initial data and conservation laws, a *shock* may arise. This is visible as a discontinuity in the solution and the fact that the characteristic lines cross each other. See Figure 1 for an example characteristic plot where a shock exists. The traveling speed of the shock is determined by the *Rankine-Hugoniot condition*

$$s(t) = \frac{f(u^+(t)) - f(u^-(t))}{u^+(t) - u^-(t)}. \tag{1.5}$$

A *rarefaction wave* is the opposite, when you have "empty" fields in your

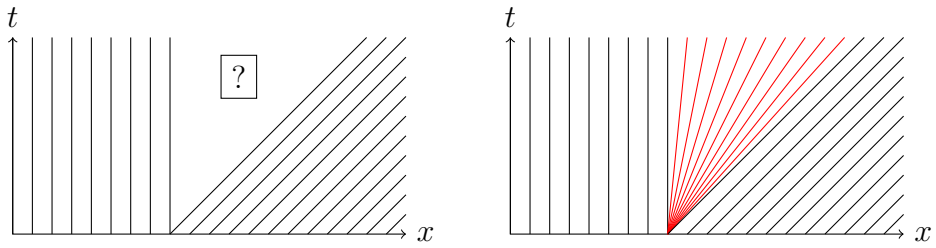

(a) A rarefaction wave with undecided characteristics in the center.

(b) A rarefaction wave satisfying the Lax entropy condition (1.4).

Figure 2: Characteristics of a rarefaction solution.

initial characteristic plot that you need to fill out, see Figure 2a for an example. Many valid weak solutions exists, but we need a unique entropy solution.

Utilizing Rankine-Hugoniot (1.5) and the Lax entropy condition (1.4) we realize the entropy solution is to "fill it out" with a fan shape starting in the origin of the rarefaction. See Figure 2b for an illustration of the entropy solution.

1.4 Finite volume scheme

In this section we will develop a finite volume scheme for the one dimensional scalar conservation law(1.3). Since equations of this type does not necessarily have continuous solutions we search for weak solutions and define control cells instead of the usual grid points. This is done because an average cell value better maps discontinuous data. For $x \in [x_L, x_R]$ we define the discrete points as

$$x_j = x_L + \left(j + \frac{1}{2}\right)\Delta x, \qquad j = 0, \ldots, N, \qquad \Delta x = \frac{x_R - x_L}{N+1},$$

and the control volumes as

$$C_j = \left[x_{j-1/2}, x_{j+1/2}\right)$$

where $x_{j\pm 1/2}$ are the midpoints between two discrete neighboring grid points. We also use a uniform discretization in time,

$$t^n = n\Delta t.$$

Since (1.3) might be discontinuous, instead of looking at point values we try to update the control cell averages instead, defined as

$$U_j^n \approx \frac{1}{\Delta x}\int_{x_{j-1/2}}^{x_{j+1/2}} u(x, t^n)dx$$

for each time step t^n. Integrating (1.3) over $x \in [x_{j-1/2}, x_{j+1/2}]$ in space and $t \in [t^n, t^{n+1}]$ in time yields

$$\int_{t^n}^{t^{n+1}}\int_{x_{j-1/2}}^{x_{j+1/2}} \partial_t u dx dt + \int_{t^n}^{t^{n+1}}\int_{x_{j-1/2}}^{x_{j+1/2}} \partial_x f(u) dx dt = 0.$$

Defining

$$F_{j+1/2}^n = \frac{1}{\Delta t}\int_{t^n}^{t^{n+1}} f(u(x_{j+1/2}), t)dt \tag{1.6}$$

this sorts itself out to

$$U_j^{n+1} = U_j^n - \frac{\Delta t}{\Delta x}\left(F_{j+1/2}^n - F_{j-1/2}^n\right). \tag{1.7}$$

In (1.6) we define flux passing in and out from a cell from time t^n to t^{n+1}. The change in U_j^n in the same timespan is only what flux through the endpoints of the interval. This means that (1.7) is a conservation statement. Since we do not know the fluxes beforehand we need to approximate them, and in here lies many of the differences in what method to approach the problem from.

Wanting to approximate (1.6), Gudonov [3] assumed that the cell averages are constant in each cell C_j and therefore the interfaces between them define a *Riemann problem*:

$$\begin{cases} \partial_t \bar{u} + \partial_x f(\bar{u}) & = 0 \qquad\qquad\qquad\qquad\qquad (x \in \mathbb{R}, \quad t > t^n) \\ \bar{u}(x, t^n) & = \begin{cases} u_j^n & \text{if } x < x_{j+1/2} \\ u_{j+1}^n & \text{if } x > x_{j+1/2}. \end{cases} \end{cases} \tag{1.8}$$

This means that our solution is a superposition of Riemann problems (1.8). Combining these solutions together we get $u(x,t) = \bar{u}(x,t)$ as long as (x,t) is reasonably close to $(x_{j+1/2}, t^n)$. The solution of the Riemann problems forms shock waves, rarefactions and compound waves. To prevent the waves from affecting each other we impose the Courant–Friedrichs–Lewy condition, also called the *CFL-condition*:

$$\max_j |f'(u_j^n)| \frac{\Delta t}{\Delta x} \leq \frac{1}{2}. \tag{1.9}$$

This can be inferred from the fact that the solution waves have a finite speed that is bounded by $\max_j |f'(u_j^n)|$. Solving each of the Riemann problems with the CFL-condition active guarantees that waves from adjacent cells do not interact.

1.5 Approximate Riemann solver

To be able to resolve rarefaction waves we will approximate a solution to the Riemann problem by using two waves: one traveling right with speed $s_{j+1/2}^l$ and one traveling left with speed $s_{j+1/2}^r$. The approximate solution to the Riemann problem (1.8) is:

$$u_0(x) = \begin{cases} u_j^n & \text{if} \quad x < s_{j+1/2}^l t \\ u_{j+1/2}^* & \text{if} \quad s_{j+1/2}^l t < x < s_{j+1/2}^r t \\ u_{j+1}^n & \text{if} \quad x > s_{j+1/2}^r t. \end{cases}$$

We determine the exact solution to the middle state using the Rankine-Hugoniot condition (1.5):

$$f(u_{j+1}^n) - f_{j+1/2}^* = s_{j+1/2}^r \left(u_{j+1}^n - U_{j+1/2}^*\right)$$
$$f(u_j^n) - f_{j+1/2}^* = s_{j+1/2}^l \left(u_j^n - U_{j+1/2}^*\right),$$

with $f_{j+1/2}^*$ being the middle flux. These equations represents a system which can be solved for $f_{j+1/2}^*$, and we take the wave speeds to be equal in magnitude but with opposite sign ($s^r = -s^l = s$) we get the simple expression

$$f_{j+1/2}^* = \frac{f(u_j^n) + f(u_{j+1}^n}{2} - \frac{s_{j+1/2}}{2}\left(u_{j+1}^n - u_j^n\right).$$

We represent the flux function by using the approximation

$$F_{j+1/2}^n \approx f_{j+1/2}^*.$$

1.6 Lax-Friedrichs scheme

The maximum allowed wave speeds are chosen to ensure neighboring Riemann problems do not interact, and the maximum allowed speeds are

$$s_{j+1/2}^l = -\frac{\Delta x}{\Delta t}, \qquad s_{j+1/2}^r = \frac{\Delta x}{\Delta t}. \tag{1.10}$$

The wave speeds (1.10) leads to the total flux function for Lax-Friedrichs scheme:

$$F_{j+1/2} = \frac{f(U_j^n) + f(U_{j+1}^n)}{2} - \frac{\Delta x}{2\Delta t}\left(U_{j+1}^n - U_j^n\right), \tag{1.11}$$

and so the full Lax-Friedrichs scheme is given by (1.7) and (1.11).

1.7 Rusanov scheme

The Lax-Friedrichs scheme uses the same wave speeds over the whole domain, which is not strictly necessary. Another scheme, the Rusanov Scheme (also called local Lax-Friedrichs) chooses the speeds based on a more local metric:

$$s_{j+1/2} = \max\left(|f'(U_j^n)|, |f'(U_{j+1}^n)|\right),$$

now assuming that $f(\cdot)$ is convex (which is not strictly needed, but makes the flux much easier to evaluate). The Rusanov method selects the wave speeds based on local data, not on the whole domain like Lax-Friedrich does. The Rusanov flux is thus given as:

$$F_{j+1/2} = \frac{f(U_j^n) + f(U_{j+1}^n)}{2} - \frac{\max\left(|f'(U_j^n)|, |f'(U_{j+1}^n)|\right)}{2}\left(U_{j+1}^n - U_j^n\right), \tag{1.12}$$

and the full Rusanov scheme is given by (1.7) and (1.12).

2 Monte Carlo methods

Monte Carlo methods are used extensively in scientific research both in physics and mathematics. This section will present the main results from the method. For a deeper understanding of the subject, Caflisch's [4] review article is excellent.

The integral of a Lebesgue integrable function $f(\omega)$ with respect to a probability density $p(\omega)$ can be expressed as

$$I[f] = \int_\Omega f(\omega)p(\omega)d\omega,$$

with $\omega \in \Omega$. The *cumulative distribution function*, or CDF, is defined as

$$P(\omega) = \int_{-\infty}^{\omega} p(u)du, \tag{2.1}$$

and the integral over the whole domain is always one. If we let ω be a uniformly distributed random variable on Ω we say that

$$I[f] = E[f],$$

so expectations can be formulated as an integral. We further define the Monte Carlo integral as

$$I_M[f] = \frac{1}{M}\sum_{m=1}^{M} f(\omega_m), \tag{2.2}$$

where $\{\omega_m\}_{m=1}^M$ is independently sampled from $p(\omega)$. According to the Strong Law of large numbers [4], this is converging with probability one, so

$$\lim_{M\to\infty} I_M[f] \to I[f].$$

We further have that the integration error is

$$e_M[f] = I[f] - I_M[f]$$

and using the Central Limit Theorem [4] we can state that for large N we have

$$e_M \approx \sigma M^{-1/2}\nu, \tag{2.3}$$

where ν is a standard normal random variable and $\sigma = \sigma(f)$ is the square root of the variance (or standard deviation) of f:

$$\sigma(f) = \left(\int_\Omega \left(f(\omega) - I[f]\right)^2 d\omega\right)^{1/2}.$$

The expectation can also be called the first moment. If $f(\omega) = f(x, t, \omega)$ we define the second moment (or two point correlation function [5]) as

$$m_2(x_i, x_j, t) = \int_\Omega f(x_i, t, \omega) f(x_j, t, \omega) p(\omega) d\omega. \tag{2.4}$$

Letting $\omega \in \Omega = \mathbb{R}^n$, all the above still holds in more dimensions and we get an error term that scales as $\mathrm{O}(M^{-1/2})$, independent of the spatial dimensionality. The convergence rate is quite slow, but the Monte Carlo method is easy to work with and therefore utilized a lot.

3 Conservation Laws with uncertain initial data

3.1 Monte Carlo Rusanov

In this section we describe a procedure for generating a numerical solution to the conservation law with uncertain initial data. We are interested in taking a look at what happens when the initial data is non-deterministic. To do this we sample the random parameter, generate initial data and send this initial data to a deterministic solver. We use this solver as a black box. We repeat this process M times. The mean value and standard deviation are calculated from the results. For the mean value we use the definition of the Monte Carlo integral (2.2), rewritten to fit this data as

$$E_M[u](x,t) = \frac{1}{M}\sum_{i=1}^{M} u_i(x,t,w), \tag{3.1}$$

where each u_i is a different realization of the problem with uncertain initial data. The second moment (2.4) is

$$m_2(x_i,x_j) = \frac{1}{M}\sum_{i=1}^{M} u_i(x_i,t)u_i(x_j,t), \tag{3.2}$$

and we also use the discrete version of the standard deviation:

$$\mathrm{SD}_M(u) = \left(\frac{1}{M}\sum_{i=1}^{M}\left(u_i(x,t,\omega) - E_M[u](x,t)\right)^2\right)^{1/2} \tag{3.3}$$

If the underlying black box solver is a Rusanov solver we call this procedure Monte Carlo Rusanov.

3.2 Uncertain shock location

We follow Schwab and Tokareva [5] and consider the following stochastic Riemann problem on the scalar conservation law (1.3)

$$u_0(x,w) = \begin{cases} u^- & \text{if } x < x_0 + Y(\omega) \\ u^+ & \text{if } x > x_0 + Y(\omega), \end{cases} \tag{3.4}$$

with ω a random variable with distribution $Y(\omega)$. We introduce the stochastic variable $y = x_0 + Y(\omega) \in \mathbb{R}$. Using the method of characteristics this can be shown to be solved by

$$u(x,t,w) = u^- + (u^+ - u^-)H(x - st - y),$$

where $H(\cdot)$ is the Heaviside function and $s = s(t)$ is the shock speed determined by the Rankine-Hugeniot condition (1.5). Given that y has the probability density $p(y)$, the expectation can be written as

$$\begin{aligned} E(x,t) &= \int_{-\infty}^{\infty} u(x,t,y)p(y)dy \\ &= u^- + (u^+ - u^-)\int_{-\infty}^{\infty} H(x-st-y)p(y)dy \\ &= u^- + (u^+ - u^-)\int_{-\infty}^{\infty} (1 - H(y-(x-st))\, p(y)dy, \end{aligned}$$

Where the last equality comes from a property of the Heaviside function. In the sense of distributions we have that $H'(y-y_0) = \delta(y-y_0)$ where $\delta(\cdot)$ is the delta function:

$$\int_{-\infty}^{\infty} \phi(y)\delta(y-y_0) = \phi(y_0)$$

for any test function $\phi(y) \in C_c^\infty(\mathbb{R})$. Putting all this together we have that the expected solution to (1.1) with initial condition (3.4) is

$$\begin{aligned} E[u](x,t) &= u^- + (u^+ - u^-)\left(1 - H(y-(x-st))\right) P(y)|_{-\infty}^{\infty} \\ &\quad + (u^+ - u^-)\int_{-\infty}^{\infty} \delta(y-(x-st))P(y)dy \\ &= u^- + (u^+ - u^-)P(x-st) \end{aligned} \tag{3.5}$$

with $P(\cdot)$ being the cumulative distribution function (2.1). Wee see that the solution varies only with the distribution of the shock location.

3.3 Example on uncertain shock location

We let the uncertain shock position be distributed with a uniform variable $c(2\mathcal{U}(\omega)-1)$ where $\mathcal{U}(\omega) \sim \mathcal{U}(0,1)$. This implies that the stochastic variable $y = x_0 + c(2\mathcal{U}(\omega)-1) \sim \mathcal{U}(x_0-c, x_0+c)$. The density and distribution function of y is now

$$p(y)) = \begin{cases} \frac{1}{2c} & \text{if } y \in [x_0-c, x_0+c] \\ 0 & \text{otherwise.} \end{cases}$$

$$P(y) = \begin{cases} 0 & \text{if } y < x_0 - c \\ \frac{1}{2c}(y - x_0 + c) & \text{if } y \in [x_0-c, x_0+c] \\ 1 & \text{if } y > x_0 + c. \end{cases}$$

Using (3.5) to solve this initial value problem we get the solution

$$
\begin{aligned}
u(x,t) &= u^- + (u^+ - u^-)P(x - st) \\
&= u^- + (u^+ - u^-) \begin{cases} 0 & \text{if } x - st < x_0 - c \\ \frac{1}{2c}(x - st - x_0 + c) & \text{if } x - st \in [x_0 - c, x_0 + c] \\ 1 & \text{if } x - st > x_0 + c, \end{cases}
\end{aligned} \tag{3.6}
$$

4 Numerical experiments

This section presents numerical examples of solving hyperbolic conservation laws with random initial data. Some of these examples are comparable to experiments done by Mishra and Schwab [6]. The examples are computed using C++ and Armadillo [7], a C++ linear algebra library. For all the numerical examples we consider Burgers' equation:

$$\begin{aligned} \partial_t u(x,t) + \partial_x \left(\frac{u^2(x,t)}{2} \right) = 0 \qquad\qquad x \in [0,1] \qquad t > 0 \\ u(x,0) = u_0(x). \end{aligned} \tag{4.1}$$

The implementation should, however, be general enough to solve other conservation laws with small amounts of modification. If the initial data is uncertain we also have a dependency on a random variable ω in some probability space Ω:

$$\begin{aligned} \partial_t u(x,t,\omega) + \partial_x \left(\frac{u^2(x,t,\omega)}{2} \right) = 0 \qquad\qquad x \in [0,1] \quad t > 0 \quad \omega \in \Omega \\ u(x,0,\omega) = u_0(x,\omega). \end{aligned} \tag{4.2}$$

For these experiments we utilize the Rusanov scheme (1.7), (1.12) as described in Chapter 1. For Burgers' equation we notice that $f(u) = \frac{1}{2}u^2$ and $f'(u) = u$. We also denote n as the number of control volumes.

4.1 Discontinuous initial data

First we will do an experiment on the deterministic Burgers Equation (4.1) using discontinuous initial data:

$$u_0(x) = \begin{cases} 1 & \text{if } x \leq 0.5 \\ 0 & \text{if } x > 0.5. \end{cases}$$

The exact solution to this problem can be calculated by using the Rankine-Hugoniot condition (1.5) to determine the shock speed:

$$s = \frac{0 - \frac{1^2}{2}}{0 - 1} = 1/2,$$

which then can be used to determine the solution

$$u(x) = \begin{cases} 1 & \text{if } x \leq 0.5 + 0.5t \\ 0 & \text{if } x > 0.5 + 0.5t. \end{cases}$$

For this experiment we used homogeneous Neumann boundary conditions and $n = 100$. Since the max value of u is 1, we set the CFL-condition (1.9) to $\Delta t = \frac{\Delta x}{2}$. In Figure 3 the initial condition and the solution after some time has passed is plotted.

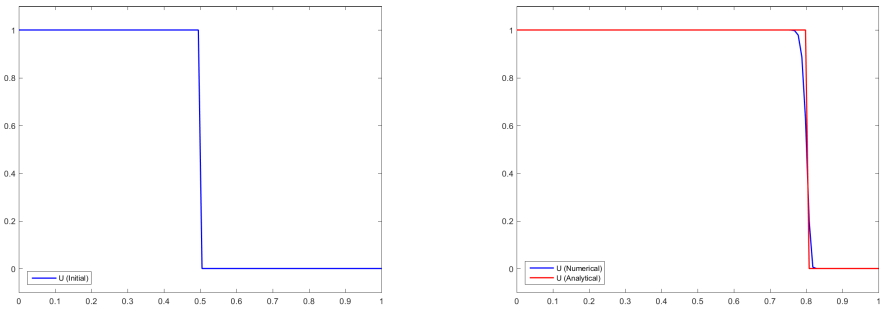

(a) $t = 0$ (b) $t = 0.6$

Figure 3: The initial condition and solution for the simple shock problem.

We see that the Rusanov method diffuses some around the discontinuity but otherwise works well. This can be (somewhat) fixed by choosing a larger n value.

4.2 Numerical Monte Carlo method

The remaining experiments we follow the procedure called Monte Carlo Rusanov described in Chapter 3.1. Unless otherwise noted we let $M = 1000$. The random numbers are generated by the Mersenne twister implemented in the C++11 standard library. The mean value (3.1) and standard deviation (3.3) for some time steps are calculated and saved to disk for inspection. The mean field is then plotted, where the mean is plotted with a line. The mean $\pm$ standard deviation is plotted with dotted lines.

4.3 Discontinuous initial data with skewed cutoff point

This experiment tests the Monte Carlo Rusanov scheme for uncertain initial data. We use initial conditions (3.4) and a uniformly distributed shock location as described in Chapter 3.3. We let $u^- = 1$, $u^+ = 0$, $c = 0.1$, $x_0 = 0.5$ and $M = 1000$. We still use $n = 100$ control cells. We plot the numerical mean solutions to (4.2) together with the expected analytical solution (3.6) in Figure 4. The standard deviation of the numerical solution is also plotted with a dotted line.

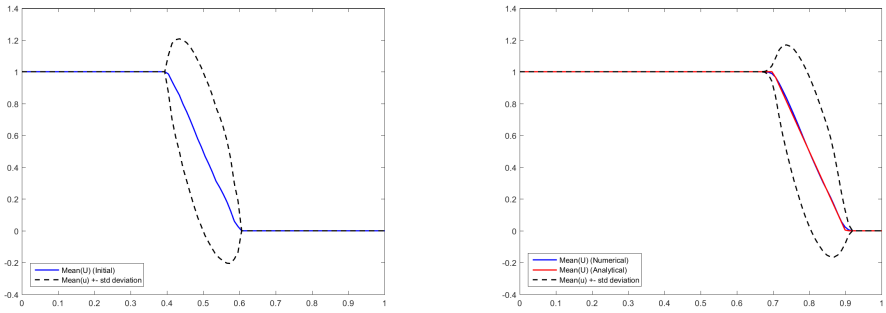

(a) $t = 0$ (b) $t = 0.6$

Figure 4: The initial condition and solution for the shock with uncertain initial position.

Interestingly enough we get a seemingly continuous function for mean(U), even though none of the individual solutions were. This is in line with the expected analytical solution.

The convergence rate was measured by taking the L^1 norm of the difference between the numerical and analytical solution. The errors are presented in Table REF. To not have the error term dominated by the Black Box error, we set $n = 1000$.

Table 1: Error table for different M using the Monte Carlo Rusanov solver

M	Error	Convergence rate
100	6.2262	
500	3.0279	-0.4479
1000	2.3546	-0.3628
2000	1.1452	-1.0399
5000	1.0829	-0.0610
10000	0.7781	-0.4769
20000	0.3018	-1.3664
100000	0.1672	-0.3699

The results are also presented as a Log-Log plot in Figure 5. The results are in line with what we expected (2.3), and it seems to converge at a rate of $M^{-1/2}$.

It would also be interesting to check whether the second moment (3.2) is continuous. The results are plotted in Figure 6. We see that the second moment also gets the smoothing effect that the first moment does. This was also observed by Schwab and Tokareva [5].

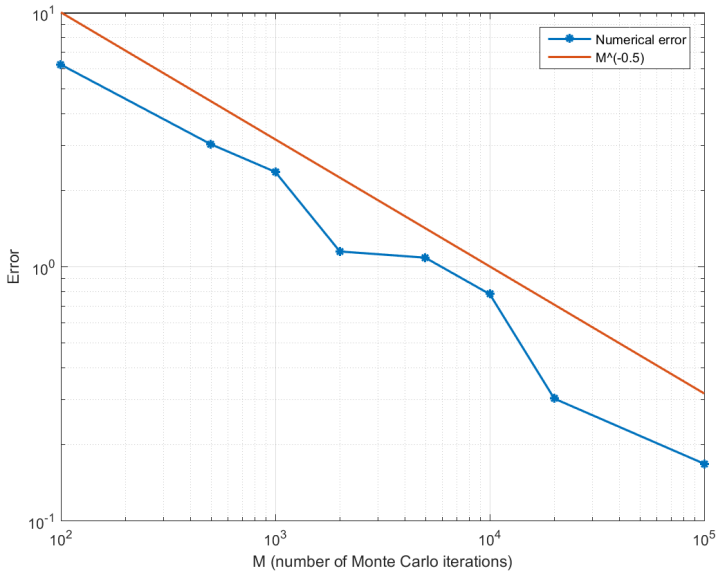

Figure 5: Log-log plot for the convergence of the Monte Carlo Rusanov solver.

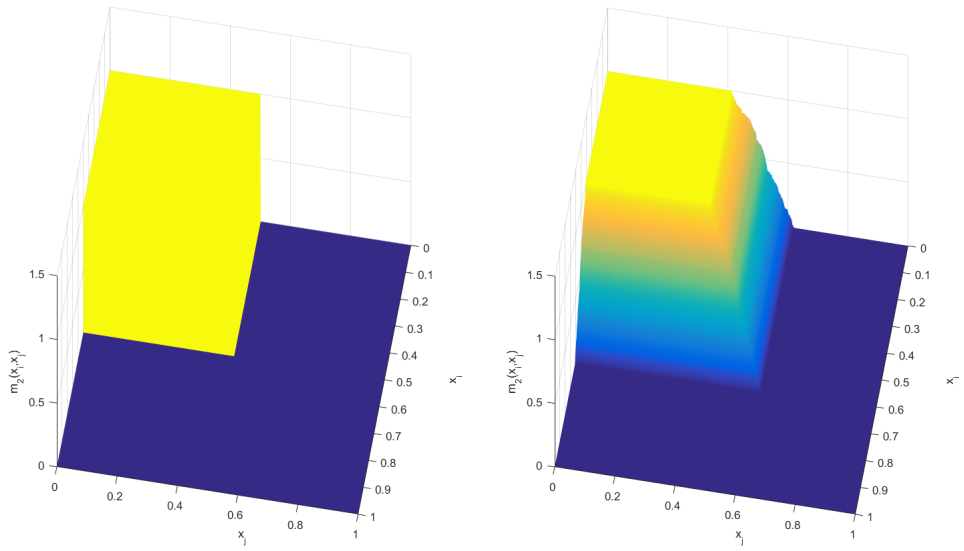

(a) Second moment of the deterministic version.

(b) Second moment of the solution to the uncertain problem.

Figure 6: The second moment of the problem with both deterministic and uncertain initial position for the shock (at time $t = 0.6$)

4.4 Discontinuous initial data with multiple Riemann problems

What happens if you try to solve multiple stochastic Riemann problems? This experiment sets up 4 different heights on the domain:

$$u_0(x,w) = \begin{cases} Y_1(\omega) & \text{if } 0 < x \leq 0.25 \\ Y_2(\omega) & \text{if } 0.25 < x \leq 0.5 \\ Y_3(\omega) & \text{if } 0.5 < x \leq 0.75 \\ Y_4(\omega) & \text{if } 0.75 < x \leq 1 \end{cases}, \quad Y_i(\omega) \sim \mathcal{U}(0,1), \quad i \in [1,2,3,4].$$

Now we solve the Riemann problems, still using the same settings as before but let $n = 1000$. However we change to use periodic boundary conditions. An example run of one initial condition can be seen in Figure 7, while the mean field results can be seen in Figure 8.

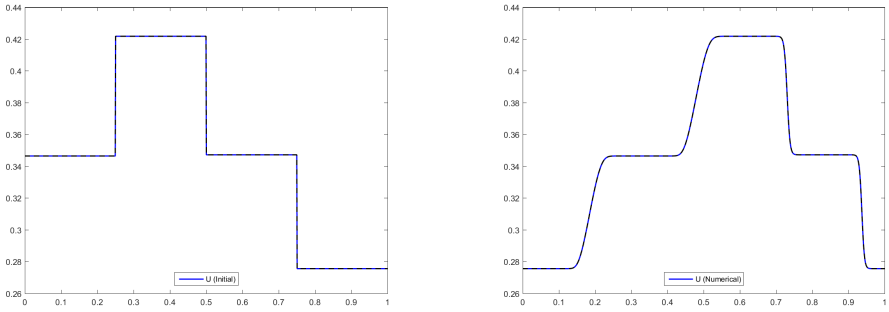

(a) $t = 0$ (b) $t = 0.6$

Figure 7: The initial condition and solution for a single problem with 4 Riemann problems.

As can be seen in Figure 8 the mean values lie close to zero in the start, but they have large variance. The mean field is disturbed at the start of the process having large local gaps, but eventually settles down with some small ripple effects.

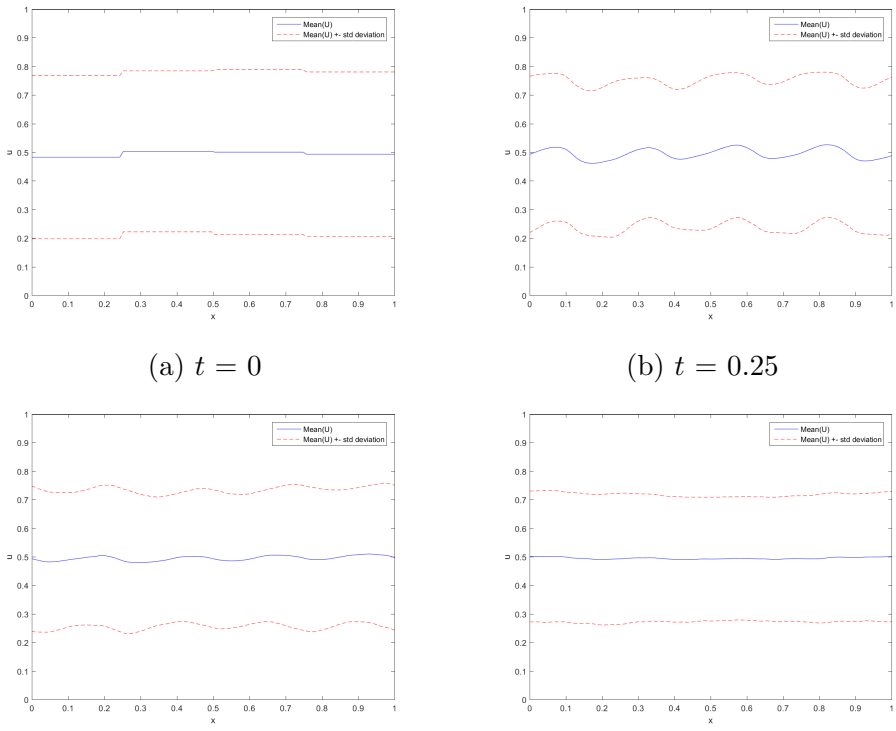

(a) $t = 0$ (b) $t = 0.25$

(c) $t = 0.5$ (d) $t = 0.75$

Figure 8: Multiple stochastic Riemann problems at times t.

4.5 Stochastic amplitude

Next up is the sine function, with uncertain amplitude:

$$u_0(x, \omega) = Y(\omega) \sin(2\pi x), \qquad Y(\omega) \sim \mathcal{U}(0, 1), \tag{4.3}$$

and the results can be viewed in Figure 9.

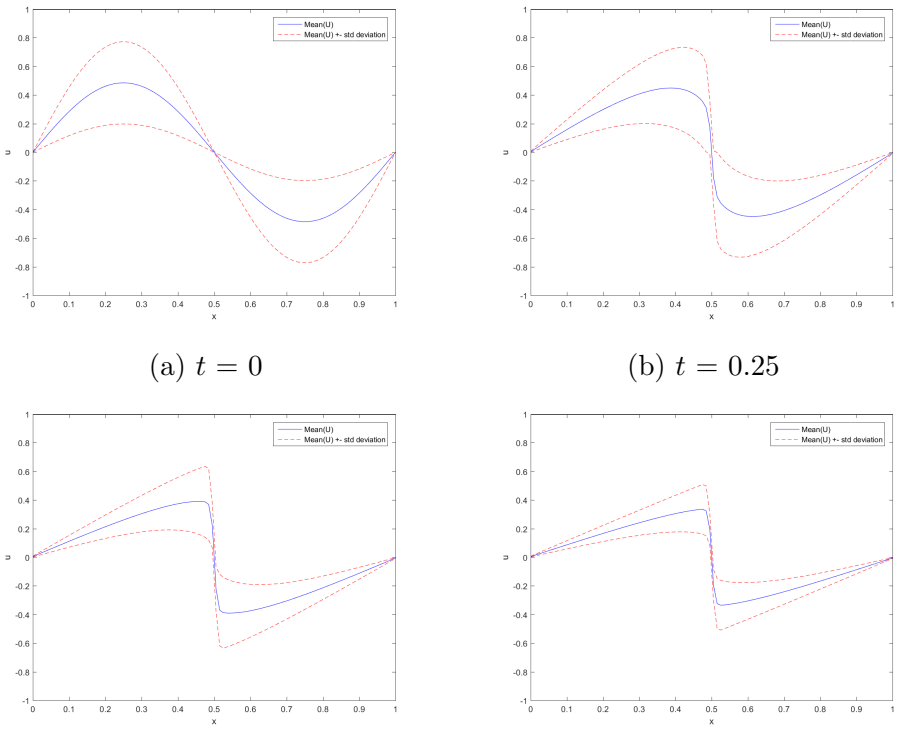

(a) $t = 0$ (b) $t = 0.25$

(c) $t = 0.5$ (d) $t = 0.75$

Figure 9: Sine with stochastic amplitude at time t

Here we observe that a stochastic amplitude means we only have uncertainty in the resulting mean field amplitude. We also register that the shock is developed in exactly the same spot for each sample and the expected solution is discontinuous.

4.6 Stochastic phase

The final experiment is a sine with an uncertainty in the phase:

$$u_0(x, \omega) = \sin(2\pi(x + 0.1Y(\omega)), \qquad Y(\omega) \sim \mathcal{U}(0, 1). \tag{4.4}$$

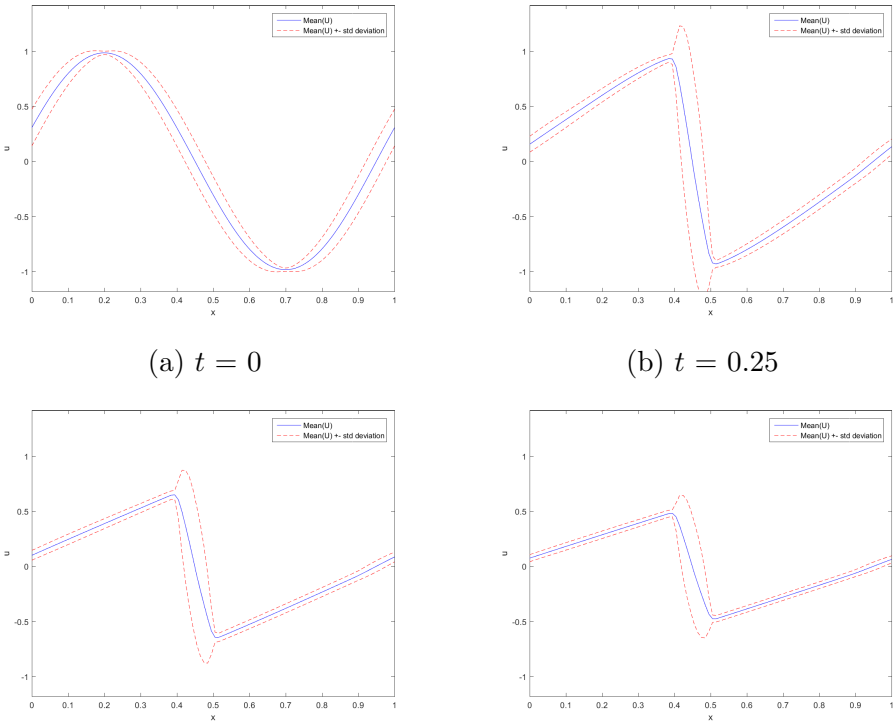

(a) $t = 0$ (b) $t = 0.25$

(c) $t = 0.5$ (d) $t = 0.75$

Figure 10: Sine with stochastic amplitude at time t

As the results in Figure 10 indicate, this solution bears resemblance to the solutions presented in Figure 4. We still get the typical sine-collapse towards the middle, but we also have a seemingly continuous mean field.

The second moment of the last two experiments could also be interesting. The results are presented in Figure 11. Also here we get a much smoother solution in the case where the first moment was smooth.

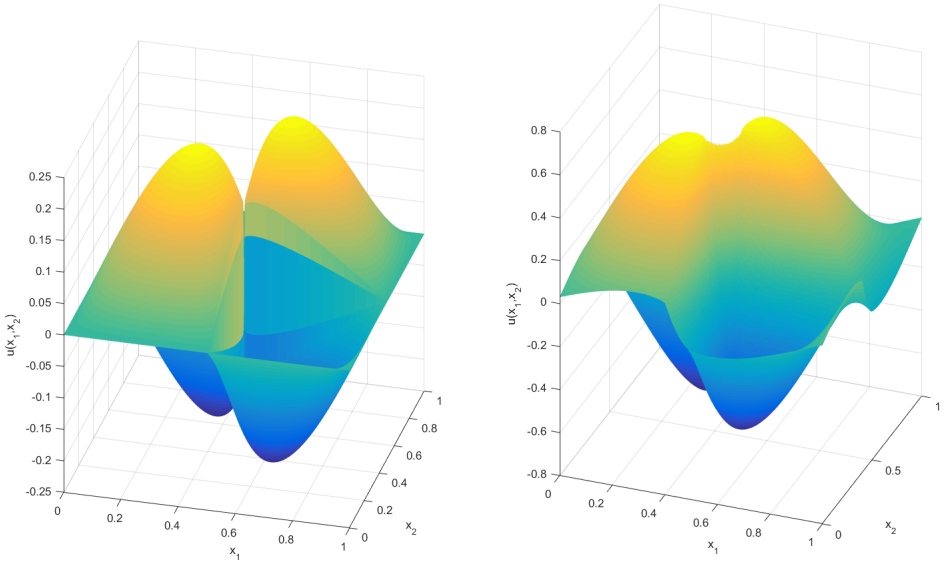

(a) Second moment of the problem (4.3).

(b) Second moment of the problem (4.4).

Figure 11: Second moment for two similar experiments

5 Conclusion and further work

We conclude that for simple scalar one dimensional conservation laws, the Monte Carlo Rusanov solver works quite well. Further work could either entail advancing into either more spatial dimensions or into systems of equations. Further work could also be directed at getting to the solution quicker, either through variation reduction methods (to get the constant solution factor smaller) or try to reduce the growth rate. One such method could be the quasi Monte Carlo method, which promises quicker run time at the cost of more preparation work. If the quasi Monte Carlo method could be fitted properly to these conservation laws, it would be interesting to analyze for what degree of stochastic dimensions the computation speed increases. The theory suggests that the quasi Monte Carlo could work well on a small to medium amount of stochastic dimensions, but at just what point it is effective could be a new experiment.

References

[1] H. Holden and N. H. Risebro. *Front tracking for hyperbolic conservation laws*, volume 152 of *Applied Mathematical Sciences*. Springer, 2011.

[2] S. Mishra. Numerical Methods for conservation laws and related equations. Lecture notes for Numerical Methods for Partial Differential Equations, ETH.

[3] S. K. Godunov. A difference method for numerical calculation of discontinuous solutions of the equations of hydrodynamics. *Matematicheskii Sbornik*, 89(3):271–306, 1959.

[4] R. E. Caflisch. Monte Carlo and quasi-Monte Carlo methods. *Acta numerica*, 7:1–49, 1998.

[5] C. Schwab and S. Tokareva. High order approximation of probabilistic shock profiles in hyperbolic conservation laws with uncertain initial data. *ESAIM: Mathematical Modelling and Numerical Analysis*, 47(03):807–835, 2013.

[6] S. Mishra and C. Schwab. Sparse tensor multi-level Monte Carlo finite volume methods for hyperbolic conservation laws with random initial data. *Mathematics of Computation*, 81(280):1979–2018, 2012.

[7] C. Sanderson. Armadillo: An open source C++ linear algebra library for fast prototyping and computationally intensive experiments. In *NICTA*, Australia, Oct 2010.